Materials Science & Engineering C 119 (2021) 111410

Contents lists available at ScienceDirect

Materials Science & Engineering C

journal homepage: www.elsevier.com/locate/msec

Bio-inspired polymeric iron-doped hydroxyapatite microspheres as a tunable carrier of rhBMP-2

Tatiana M. Fernandes Patrício[a,*], Didem Mumcuoglu[b,c], Monica Montesi[a], Silvia Panseri[a], Janneke Witte-Bouma[d], Shorouk Fahmy Garcia[c,e], Monica Sandri[a], Anna Tampieri[a], Eric Farrell[d,1], Simone Sprio[a,*,1]

[a] Institute of Science and Technology for Ceramics, National Research Council, Faenza, Italy
[b] Fujifilm Manufacturing Europe B.V., Tilburg, the Netherlands
[c] Department of Orthopaedics, Erasmus MC, University Medical Center Rotterdam, the Netherlands
[d] Department of Oral and Maxillofacial Surgery, Special Dental Care and Orthodontics, Erasmus MC, University Medical Center Rotterdam, the Netherlands
[e] Department of Internal Medicine, Erasmus MC, University Medical Centre Rotterdam, the Netherlands

ARTICLE INFO

Keywords:
Hybrid superparamagnetic microspheres
Osteogenesis
rhBMP-2
Sustained release
Pulsed electromagnetic field
Bone regeneration

ABSTRACT

Hybrid superparamagnetic microspheres with bone-like composition, previously developed by a bio-inspired assembling/mineralization process, are evaluated for their ability to uptake and deliver recombinant human bone morphogenetic protein-2 (rhBMP-2) in therapeutically-relevant doses along with prolonged release profiles. The comparison with hybrid non-magnetic and with non-mineralized microspheres highlights the role of nanocrystalline, nanosize mineral phases when they exhibit surface charged groups enabling the chemical linking with the growth factor and thus moderating the release kinetics. All the microspheres show excellent osteogenic ability with human mesenchymal stem cells whereas the hybrid mineralized ones show a slow and sustained release of rhBMP-2 along 14 days of soaking into cell culture medium with substantially bioactive effect, as reported by assay with C2C12 BRE-Luc cell line. It is also shown that the release extent can be modulated by the application of pulsed electromagnetic field, thus showing the potential of remote controlling the bioactivity of the new micro-devices which is promising for future application of hybrid biomimetic microspheres in precisely designed and personalized therapies.

1. Introduction

Bone tissue regeneration is a complex biologic process that, in the case of critical-size defects, cannot proceed spontaneously. The tissue regeneration must be supported by the implantation of devices, engineered to mimic the extracellular matrix (ECM) and provide a physicochemical environment favouring osteoblast differentiation and new bone formation. A major approach is the use of hydroxyapatite, combined with biopolymers such as collagen or chitosan to give bone-like hybrid composition and, also, endowed with the ability to release bioactive factors, to trigger and sustain the bone regenerative cascade [1–5]. Human bone morphogenetic protein (BMP-2) is among the most investigated growth factor in clinical trials [6–8]. In spite of previous in vitro and in vivo studies have shown that hydroxyapatite and, particularly, hybrid materials, have a good ability to link biomolecules with a better effect on cell adhesion, proliferation and osteoblastic differentiation [9–11]. A still open challenge is to develop release mechanisms able to be controlled over time, to prevent the administration of supra-physiological BMP-2 doses, which can result in severe side effects (e.g. oedema, bone malformations, cancer) [5,7,10]. Among possible activation methods, the use of magnetic fields has been used in recent years to enhance the regenerative process by direct magnetic stimulation or by modulation of the osteogenic character or the drug release ability [12,13]. Several approaches have produced magnetic biomaterials by incorporation of iron oxide nanoparticles into bovine extracted hydroxyapatite [14], or synthesis of magnetite/apatite [15], or by adding M-type ferrite to hybrid materials [16], or to prepare magnetic hydroxyapatite coating by soaking magnetic bioglass in simulated body fluid [17]. On the other hand, intrinsically magnetic apatite nanophase (Fe-HA) has been recently developed by partial substitution of Ca^{2+} ions with Fe^{2+}/Fe^{3+} ions [18,19]. This novel biomaterial is characterized by excellent biocompatibility and

* Corresponding authors.
E-mail addresses: tatianamfp@gmail.com, tatiana.patricio@ipleiria.pt (T.M. Fernandes Patrício), simone.sprio@istec.cnr.it (S. Sprio).
[1] Principal Investigator.

https://doi.org/10.1016/j.msec.2020.111410
Received 11 May 2020; Received in revised form 3 August 2020; Accepted 16 August 2020
Available online 22 August 2020
0928-4931/

enhanced osteogenic ability. It has been previously combined with natural (e.g. gelatine, collagen) or synthetic polymers (e.g. polylactic acid, poly ε-caprolactone) or recombinant proteins (e.g. RCP), to produce bone-mimicking devices with superparamagnetic properties and capable of promoting good cell viability, adhesion and spreading, as well as osteogenic induction in vitro [2,20–26] and new bone formation in vivo [27]. Recent studies showed that Fe-HA phase can be heterogeneously nucleated on a collagen I based recombinant peptide (RCP), thus obtaining a bio-hybrid compound with bone-like composition, then engineered into microspheres by an emulsification process and characterized for their cytocompatibility and osteogenic ability in presence of MC3T3-E1 cell line from mouse [25,26]. Therefore, remains the challenge on developing suitable bone scaffolds as carrier of relevant drugs, growth factors or biomolecules to sustain the regenerative cascade.

To best of our knowledge, no scientific reports have shown the investigation of magnetic bio-inspired and bone-like microspheres as potential carrier of therapeutic factors for bone tissue applications. Herein, the viability of using bio-inspired and magnetic microspheres in the presence of human paediatric mesenchymal stromal cells (hMSCs) and as a carrier of rhBMP-2 was investigated to address innovative therapies for bone regeneration. The microspheres were subjected to physicochemical, morphological and biological characterization and evaluation of adsorption efficiency, interaction with rhBMP-2 and bioactivity. In particular, analysis of cell viability and osteogenic differentiation as induced by the composition of the magnetic microspheres was performed with hMSCs in comparison with non-mineralized microspheres (i.e. obtained by RCP alone) and with microspheres mineralized with a non-magnetic hydroxyapatite phase, selected as control. The effect of the microsphere's composition on rhBMP-2 release profile was investigated for up to 14 days. Furthermore, we attempted to modulate the release profile of rhBMP-2 from the magnetic microspheres by using a low-frequency pulsed electromagnetic field (PEMF), as a proof of concept for magnetically-activated drug delivery systems and, further to be tested as relevant mechanism for cells stimulation to boost the bone tissue regeneration.

2. Experimental section

2.1. Materials

RCP is commercially available as Cellnest™ (Fujifilm Manufacturing B.V., Tilburg, The Netherlands), characterized by the molecular weight of 51.7 kDa and isoelectric point of ≈10.02 (pH ≈ 9). fluidMAG-CT (i.e. commercial magnetite nanoparticles, size 50 nm) was purchased in Chemicell (Berlin, Germany). rhBMP-2 and fluorescent rhBMP-2 (Texas red rhBMP-2) were kindly provided by Fraunhofer Institute for Interfacial Engineering and Biotechnology (Wurzburg, Germany). All the other reagents were described in the following sections. Ultrapure water (0.22 mS, 25 °C) was used in all the experiments.

2.2. Production of microspheres

Hybrid microspheres made of RCP mineralized with undoped hydroxyapatite (hereinafter coded as RCPHA) or with iron-doped hydroxyapatite (hereinafter coded as RCPFeHA) were obtained by a biomineralization process followed by water-in-oil emulsification method, as described in [26]. Briefly, 20 g of mineralized RCP slurry (obtained by biomineralization process) was dropped in 45 g of pre-warmed corn oil and kept under mechanical stirring for 20 min. The as-obtained mixture was cooled, until microspheres gelation, and dropped into a 300 mL of chilled acetone and kept under mechanical stirring for 5 min, then maintained for 1 h at room temperature, under mechanical stirring. The microspheres were left to sediment and acetone was carefully removed, then 300 mL of clean acetone was added and the microspheres were washed for 10 min. This step was repeated twice. The microspheres were filtered, dried overnight in an oven at 40 °C, and sieved to achieve a size distribution within the range of 50 to 75 μm. Three different batches of each type of microspheres were produced. By using similar emulsification method, non-mineralized RCP microspheres (hereinafter coded as RCP) were prepared, starting from RCP solution, and also microspheres made of RCP added with commercial magnetic nanoparticles (i.e. RCPfluidMAG-CT) were also produced as control materials. Then, all the obtained microspheres were crosslinked by using dehydrothermal treatment (DHT), carried out by placing the dried microspheres in glass vials covered with aluminum foil and heated at 160 °C for 48 h under vacuum. In a previous study (Fernandes Patrício et al., 2019) it was shown that the DHT treatment does not compromise the thermal, chemical, and magnetic properties of the microspheres [26].

2.3. Physicochemical and morphological characterization of the microspheres

The microspheres' cross-sections were inspected by Scanning Electron Microscope (SEM) (FEI Quanta 600, USA) in low vacuum mode with an accelerating voltage of 10 kV and a working distance of 10 mm. The samples were prepared as follows: A predetermined amount of microspheres were placed in a warm solution of agarose (2 wt%) and left to solidify, then they were introduced in the sample holder and embedded with H-OCT compound (Histo-Line Laboratories, Italy). Sliced samples (30 μm thickness) were obtained by using a microtome cryostat (5000 MC, Histo-Line Laboratories, Italy). Moreover, RCPFeHA microspheres were also analysed by using Field Emission Scanning Electron Microscopy (FE-SEM, Zeiss Sigma). Ca, P and Fe distribution was evaluated by microanalysis with Energy Dispersive Spectroscopy (EDS; Oxford X-Act with 10 mm^2 silicon drifted detector (SDD)) and INCA microanalysis Suite software.

The surface charge of microspheres was evaluated in HEPES buffer (i.e. 0.01 M; pH 7.4) at microsphere concentrations of 1.2 mg/mL, containing 12 μg/mL of rhBMP-2. All the measurements were performed with disposable folded capillary cells (DTS1061; Malvern, UK) at 25 °C in ζ-potential Zetasizer Nano analyzer (Malvern, UK). The experiment was carried out in triplicate (100 runs each) and the results were showed as Mean ± SEM.

The contact angle measurements of the as-investigated microspheres were carried out by the optical contact angle system stabilized with a camera (Contact angle, Drop shape analyzer with IDS camera, Kruss GmbH, Germany). Briefly, to have a suitable surface for the execution of the test a pellet of each type of materials was obtained by pressing ≈ 150 mg of microspheres at 100 mbar, then deionized water droplets (2 μL) were carefully dropped onto the pelletized microspheres. The contact angle was calculated by applying the fitting method (tangent) with approximation by using Kruss advance software (Kruss GmbH, Germany). The results were showed as Mean ± SEM.

The swelling behaviour was evaluated by soaking a predetermined amount of microspheres in PBS at 37 °C for 24 h. At selected time points (i.e. 1 h, 3 h, 6 h, 9 h, and 24 h) the swollen microspheres were observed by an inverted Nikon Ti-E microscope (Nikon Corporation, Tokyo, Japan) and analysed by Image J (NIH image, USA). The swelling extent in percentage (Sw, %) was calculated according to the following equation,

$$Sw = \left(\left(\frac{D_s}{D_d}\right) - 1\right) \times 100 \quad (1)$$

where, D_s and D_d are the diameter of the swollen and dried microspheres, respectively. The data were obtained by assuming a spherical shape and measuring the area of microspheres (acquired by Image J, NIH image, USA) to obtain the diameter of the microspheres. The results were showed as Mean ± SEM.

The total porosity of RCPFeHA microspheres was determined by

mercury intrusion porosimetry and was carried out within the 0–200 MPa pressure range (Pascal 140/240 series porosimeter, Thermo Finnigan, USA).

2.4. Cell culture

Human paediatric mesenchymal stromal cells (hMSCs) were isolated from surplus iliac crest material of paediatric patients (9–13 years old) undergoing cleft palate reconstruction surgery (the use of this surplus material was ethically approved (MEC-2014-16, Erasmus MC, Rotterdam, The Netherlands)). The bone chips were washed with αMEM (Minimal Essential Medium alpha, supplemented with 10% *v*/v heat-inactivated FCS (lot 41Q2047K), 50 μg/mL gentamycin and 1,5 μg/mL fungizone (all from Invitrogen, California, USA). Once the bone chips were clear of cells, the medium was transferred to T75 flasks in a total of 10 mL per flask, and 1 ng/mL fibroblast growth factor (FGF-2, Instruchemie B.V., Delfzijl, The Netherlands) and 25 μg/mL of L-ascorbic acid 2-phosphate (Sigma-Aldrich, St. Louis, USA) were added. Cells were washed thrice after 24 h of culture with PBS supplemented with 2% *v*/v FCS to remove non-adherent cells and erythrocytes. The hMSCs were cultured at 37 °C, 5% CO_2 in a humidified atmosphere. Cells from the fourth or fifth passage were used for these experiments. Three independent Donors coded as Donor 1, Donor 2 and Donor 3 were investigated.

hMSC viability was investigated in the presence of RCP, RCPHA and RCPFeHA microspheres by following two strategies: cell monolayer and 3D template (i.e. a mix of cells and microspheres).

2.4.1. Cell seeding in monolayer (cell monolayer)

hMSCs (P5) were detached near confluence (i.e. 80–90%) with 0.25% trypsin (Invitrogen, California, USA) and washed in complete αMEM. The hMSCs were re-suspended in the standard cell culture medium, as previously described [28], and were cultured at a density of 3000 cells/cm^2 in a 12-well plate. Cells were left to adhere to the well plate for 24 h, and then 500 μg of each type of microspheres were added on top of the cells. Moreover, cells only were seeded in the same conditions and were used as a control. The cell culture was kept for 7 days at 37 °C, 5% CO_2 in a humidified atmosphere. Samples were analysed by optical microscope and were treated with Live/Dead assay, for further cell viability evaluation (section Cell viability and proliferation).

2.4.2. Cell seeding strategy on microspheres (3D template)

500 μg of each type of microspheres were mixed in 2 mL Eppendorf tubes and 350 cells/cm^2 were seeded on the top of the microspheres, then cells and microspheres were mixed by inversion every 10 min for 1 h. Subsequently, cells and microspheres were left to sediment and standard cell medium was collected and replaced three times, completing another hour (Fig. 1). After 2 h of seeding, cells and microspheres were placed in the well plates covered with agarose. Cell culture was kept at 37 °C in a humidified incubator at 5% CO_2. The obtained samples were denominated as 3D templates. Triplicates of microspheres were prepared, and the results were shown as mean of standard deviation (Mean ± SD).

2.4.3. Cell viability and proliferation

2.4.3.1. Live & dead assay. Live/Dead® viability/cytotoxicity kit for mammalian cells (Life Technologies, California, USA) was performed according to the manufacturer's instructions. Briefly, the cell medium was recovered from cells seeded on 12-well plates or from RCPFeHA 3D template (in 24-well plate) and were washed once with saline solution (i.e. 0.9% *w/v* NaCl in milli-Q water), then were incubated with Live/Dead solution composed of Calcein acetoxymethyl (Calcein AM) and Ethidium homodimer-1 (EthD-1) (e.g. 1 mL of saline solution with 1 μL of Calcein AM and 1.5 μL of EthD-1), and incubated for 40 min at 37 °C, 5% CO_2 in a humidified atmosphere. Live/Dead solution was removed, and samples were washed twice with saline solution. Samples were kept in saline solution during the viability analysis with fluorescent microscope Zeiss Axiovert 200 M, with Axiovert software (Germany). Three samples per group were analysed.

2.4.3.2. DAPI staining. 3D templates were placed in a 24-well plate and 1 mL of formalin (4%) was added to fix the cells for 1 h at room temperature. 3D templates were washed three times with PBS; then were stained 5 min with DAPI solution (0.1 μg/mL) and were washed three times with PBS. The images were acquired by using fluorescent microscope Zeiss Axiovert 200 M, with Axiovert software (Germany).

2.4.3.3. DNA assay. At predetermined time points (i.e. 2 h, 1 day, 3 days, 7 days and at the end of the experiment), samples were collected and washed with PBS. Samples were digested in 300 μL papain buffer (0.1 M of sodium phosphate monobasic (≥99.0%, Sigma Aldrich, St. Louis, U.S.A) and 0.005 M of ethylenediaminetetraacetic acid disodium salt dihydrate (EDTA, Sigma Aldrich, St. Louis, U.S.A), pH 6.0, supplemented with 0.01 M of cysteine HCL (Sigma Aldrich, St. Louis, U.S.A) and 250 μg/mL of papain (Sigma Aldrich, St. Louis, U.S.A)) and incubated for 16 h at 60 °C, then the samples were mixed and incubated for another hour at 60 °C. DNA assay with ethidium bromide was used to determine the DNA amount in the samples. Samples and aliquots for the calibration curve (0–1.25 μg of Deoxyribonucleic acid sodium salt from calf thymus (DNA)) were pipetted in duplicate in a 96-well plate (50 μL), RNA was digested for 30 min at 37 °C with 0.05 mg/mL Ribonuclease type IIIa (Sigma Aldrich, St. Louis, USA) and 8,3 IU/mL Heparin in PBS. Then 25 μg/mL ethidium bromide (Thermo Fischer Scientific, Massachusetts, USA) was added and fluorescence was read with the Wallac victor (excitation 340 nm, emission 590 nm). The results were expressed as Mean ± SD in the same donor and were plotted as Mean ± SD from three independent donors ($n = 3$). The percentage of cells adhering to the microspheres (CellMS, %) was calculated, as follows:

$$Cell_{Ms} = \left(\left(\frac{DNAq}{8.5} \right) \Big/ N^{\circ}_{seed} \right) \times 100 \quad (2)$$

where, *DNAq* was the DNA quantified by the DNA assay and was

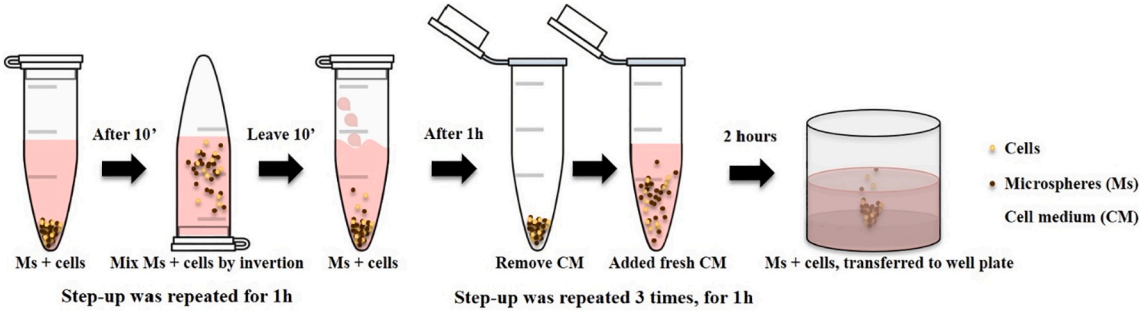

Fig. 1. Steps of cell seeding strategy to obtain 3D template.

expressed in pg; 8.5 was the DNA amount in each cell, pg [29] and N°_{seed} was the initial cells number seeded in each type of microspheres.

2.4.4. Gene expression

2.4.4.1. RNA isolation and DNA synthesis. Samples were transferred to 1.5 mL Eppendorf, washed once with PBS and were snap freezing with liquid nitrogen. RNA was isolated from the 3D templates or cells monolayer by homogenizing samples with an Eppendorf-potter in 350 μL of Trizol (Thermo Fisher Scientific, Massachusetts, USA). The total RNA was extracted by adding 70 μL of chloroform (Sigma Aldrich, St. Louis, U.S.A) and three phases after centrifugation were formed. RNA was collected from the top layer and an equal volume of 70% *v*/v of ethanol (Sigma Aldrich, St. Louis, U.S.A) was added. The RNA was purified by using RNeasy Mini Kit with RNeasy MinElute spin columns (Qiagen, Hilden, Germany), following the manufacturer's instructions and total RNA was quantified by spectrophotometry (NanoDrop 2000, Thermo Scientific, The Netherlands) at a wavelength of 260 and 280 nm. 300 ng of RNA was reverse transcribed into complementary DNA (cDNA) by using the RevertAid First Strand cDNA Synthesis kit (Thermo Fisher Scientific, Massachusetts, USA), according to the manufacturer's protocol.

2.4.4.2. Quantitative PCR. Osteogenic gene transcriptions were quantified on Bio-Rad CFX thermal cycler (Bio-RAD, California, U.S.A). Thermocycler conditions comprised an initial holding at 95 °C for 10 min, followed by one step at 95 °C for 15 s and 60 °C for 60 s for 40 cycles. For gene expression tests, three different housekeeping genes were evaluated, such as Ubiquitin C (UBC), Glyceraldehyde-3-phosphate dehydrogenase (GADPH) and Beta-2-microglobulin (B2M), while the investigated osteogenic genes were Collagen type I (COL I) and Osteonectin (SPARC). UBC and B2M mRNA levels were analysed with qPCR™ Mastermix Plus for SYBR® Green I (Eurogentec Nederland B.V., Maastricht, The Netherlands), while GADPH, COL I and SPARC, TaqMan Master Mix (Applied Biosystems, California, USA) was applied, according to the manufacturer's instructions. The as-corresponding primers were described in Table 1 [30–32]. The CT values of the housekeeper genes GADPH, B2M and UBC were averaged by using geometric averaging of every sample. This average is the best keeper index (BKI) for every single sample. All separate CT values were corrected to the BKI by using the $2^{-\Delta CT}$ formula [31]. Values were represented as Mean ± SD for samples from three independent Donors ($n = 3$) or were plotted as Mean ± SD in each Donor.

2.4.5. Preparation of histology samples

Samples were fixed in 4% formaldehyde (Klinipath, The Netherlands) in PBS, embedded in 2% w/v agarose (Eurogentec, Belgium) and subsequently processed in paraffin for light microscopy. The samples were cut into 5 μm sections by using a microtome (Leica RM 2135).

2.4.5.1. Haematoxylin and eosin staining (H&E). Pre-treated paraffin sections were deparaffinised in Xylene (2 times, 5 min each) and in 100% (2 times, 5 min each), 96% (1 time, 5 min) and 70% (1 time, 5 min) of ethanol, then were washed twice with distilled water for 3 min each. Sections were transferred to haematoxylin solution (Sigma Aldrich, St. Louis, U.S.A) for 20 s and washed with running tap water for 10 min, then were immersed in eosin Y solution (2% in 50% of ethanol and 0.5 mL of glacial acetic acid, Merck, Darmstadt, Germany) during 45 s. By the end, the sections were introduced in 70% of ethanol (10 s) and dehydrate one minute in each step, in 96% and 100% ethanol and two times in o-xylene (Sigma Aldrich, St. Louis, U.S.A). The stained sections were mounted with Depex mounting medium (Merck, Darmstadt, Germany) and analysed on an optical microscope.

2.5. In vitro loading and release of rhBMP-2

rhBMP-2 was loaded on the microspheres by adsorption method and the experimental setup was adapted from [8]. Briefly, in 1.5 mL Eppendorf LoBind tubes, 50 μL or 75 μL of predetermined concentrations (i.e. 18 μg/mL and 12 μg/mL, respectively) of rhBMP-2 were pipetted on the top of 15 mg of microspheres. This range was selected as the most suitable volume to observe the complete adsorption of the water in all the tested materials. Soluble rhBMP-2 was used as a control. All as-prepared samples were overnight incubated at 4 °C, to allow the complete adsorption of rhBMP-2 on microspheres during the swelling process.

After overnight of rhBMP-2 adsorption, a predetermined volume of supplemented DMEM (Dulbecco's Modified Eagle's Medium (DMEM), supplemented with 1% bovine serum albumin (BSA) and 1% penicillin-streptomycin (100 U/mL–100 μg/mL)) was added on the top of the microspheres (i.e. 950 μL in RCP and RCPfluidMAG-CT and 925 μL in RCPHA and RCPFeHA). A final concentration of 900 ng/mL or 400 ng/mL of rhBMP-2 was achieved.

For the release studies, samples were incubated at 37 °C, under three different conditions: agitation (≈100 rpm), static and PEMF. At given time points up to 14 days, the DMEM containing released rhBMP-2 was collected after centrifugation (3000 rpm for 5 min) and was replaced by fresh supplemented DMEM (900 μL).

After 14 days, the supernatant was collected and 900 μL of urea solution (6 M) was added to the microspheres and incubated for 4 h at 37 °C [33]. This supernatant was collected by centrifugation and dialyzed with a cellulose membrane (3500 D, Medicell Membranes Ltd., UK), for 3 days at 4 °C. milli-Q water was replaced twice a day for the complete removal of the salt. Meanwhile, all the microspheres were washed twice with PBS and the supernatant was collected for further analysis. Microspheres and soluble rhBMP-2 were digested by using 10 mg/mL of collagenase solution in DMEM and incubated two days at 37 °C. All the supernatants (supplemented DMEM with released rhBMP-2) were further analysed by sandwich enzyme-linked immunosorbent assay (ELISA) development kit specific for rhBMP-2 (PeproTech, New Jersey, USA), as described by the manufacturer's guidelines. The concentration of unknown released rhBMP-2 was quantified concerning rhBMP-2 standard calibration curve (ranging from 47 to 3000 pg/mL) run on the same plate, while the percentage of released rhBMP-2 was calculated for the positive control (soluble rhBMP-2, at a concentration of 900 or 400 ng/mL). Three samples of each group were investigated, and the amount or percentage of released rhBMP-2 was expressed as Mean ± SEM.

Table 1
Primers sequences used to define the osteogenic expression of the genes.

		Forward	Reverse
Housekeeping genes	GADPH	ATGGGGAAGGTGAAGGTCG	TAAAAGCAGCCCTGGTGACC
	UBC	ATTTGGGTCGCGGTTCTTG	TGCCTTGACATTCTCGATGGT
	B2M	5′-TGCTCGCGCTACTCTCTCTTT-3′	5′-TCTGCTGGAT GACGTGAGTAAAC-3′
Osteogenic genes	COL I	CAGCCGCTTCACCTACAGC	TTTTGTATTCAATCACTGTCTTGCC
	SPARC	ATCTTCCCTGTACACTGGCAGTTC	CTGGGTGTGGGAGAGGTACC

2.5.1. Loading efficiency of microspheres

2.5.1.1. Quantitative efficiency. To evaluate the loading efficiency of all the tested microspheres, a predetermined amount of rhBMP-2 was adsorbed on 15 mg of microspheres and kept overnight at 4 °C. Further, milli-Q water was added to the microspheres to obtain a final concentration of 900 ng/mL of rhBMP-2 and then washed three times with milli-Q water. At each washing step the milli-Q water was collected by centrifugation (3000 rpm, 5 min) and the non-adsorbed rhBMP-2 was evaluated by ELISA development kit. The percentage of loading efficiency (LE, %) of 15 mg of microspheres was calculated, as follows:

$$LE = \left(\frac{Sol_{rhBMP2} - Sum_{nads\ rhBMP2}}{Sol_{rhBMP2}}\right) \times 100 \quad (3)$$

where, Sol_{rhBMP2} is the amount of soluble rhBMP-2 and $Sum_{nads\ rhBMP2}$ is the sum of the amounts of non-adsorbed rhBMP-2 found in each washing step. The as-showed data were acquired in triplicate and presented as Mean + SEM.

2.5.1.2. Qualitative efficiency. To further identify the rhBMP-2 adsorption efficiency from RCP, RCPHA, and RCPFeHA, the predetermined concentration of texas red rhBMP-2 was adsorbed by the microspheres overnight at 4 °C. Meanwhile, the control samples were non-loaded microspheres, where the solution of rhBMP-2 was substituted by milli-Q water. Further, 825 μL or 850 μL of milli-Q water was added to the microspheres to reach a final rhBMP-2 concentration of 900 ng/mL. Non-adsorbed rhBMP-2 was removed by centrifugation (3000 rpm, 5 min) and washed three times with milli-Q water. Fluorescent images from non-loaded microspheres, loaded microspheres with 900 ng/mL of rhBMP-2 and washed microspheres were acquired by Inverted Ti-E fluorescence microscope (Nikon) with appropriate filter (i.e. excitation of 557 nm and emission of 576 nm) at equal exposure time.

2.5.2. FTIR analysis of rhBMP-2 and microspheres

To evaluate the intermolecular interaction of rhBMP-2 with all the tested microspheres ($n = 3$), the previously washed samples were freeze-dried (0.1 mbar) and evaluated by Fourier Transform Infrared Spectroscopy (FTIR) (Avatar 320 FT-IR, Thermo Nicolet, Canada). The infrared spectra were collected in the wavelength range from 400 to 4000 cm^{-1}, using the KBr pellet technique with 2 cm^{-1} of resolution. The sample (~2 mg) was mixed with ~150 mg of anhydrous KBr and the powder pressed at 8000 psi into 7 mm diameter discs. The relevant vibration modes were analysed by deconvolution and curve fitting technique (Fit by Sum with Lorentzian curve) by using MagicPlot Student 2.5.1 software.

2.5.3. In vitro rhBMP-2 bioactivity assay

rhBMP-2 bioactivity was investigated by using the C2C12 BRE-Luc bioassay cell line. To generate the BMP reporter cell line, C2C12 cells (immortalized mouse myoblast cell line) were stably transfected with pGL3(BRE)-luciferase reporter construct, as reported in [34,35] and were denominated as C2C12 BRE-Luc cell line.

The C2C12 BRE-Luc cell line was incubated in complete growth medium (i.e. Dulbecco's modified Eagle's medium without phenol (DMEM) containing 10% of foetal calf serum (FCS), 1% penicillin-streptomycin (100 U/mL–100 μg/mL) and 1 mM Sodium Pyruvate), then 200 μg/mL of Geneticin (G418, Thermo Fisher Scientific, Massachusetts, USA) was added after 4 h of plating the cells. Cells were cultured at 37 °C in a humidified incubator at 5% CO_2. Cells were detached from culture flasks by trypsinisation, centrifuged (i.e. 10 min at 250 g) and re-suspended. Cell number and viability were assessed by trypan blue dye exclusion test. For the rhBMP-2 reporter assay, investigations on rhBMP-2 release were carried out at a final concentration of 900 ng/mL, by following the adsorption assay as mentioned in the section "2.5 *In vitro* loading and release of rhBMP-2". The as-used microspheres were previously sterilised by autoclave. The used release medium was a growth medium of the C2C12 BRE-Luc cell line and the experiments were performed at 37 °C in an atmosphere of 5% CO_2. C2C12 BRE-Luc cells (≤P19) were seeded into white-walled 96-well culture plates at a density of 10,000 cells per well in 50 μL of complete growth medium. After 30 min, 50 μL of growth medium with released rhBMP-2 from RCP, RCPHA and RCPFeHA, growth medium with soluble rhBMP-2 for the controls (900 ng/mL) and standard calibration curve with soluble rhBMP-2 (900 ng/mL to 1.6 ng/mL), were added to the well plate in duplicate and incubated for 24 h at 37 °C in an atmosphere of 5% CO_2. Furthermore, lysis reconstitution buffer and lyophilized luciferin (Steady Lite Plus, Perkin Elmer Inc., Massachusetts, USA) were combined and 100 μL was added to each well. The plate was shaken for 15 min in the dark and then the luminescence signal generated by luciferin was measured 6 s by using a Wallac VICTOR Multilabel reader (Perkin Elmer Inc., Massachusetts, USA). The percentage of rhBMP-2 bioactivity (BB, %) was calculated by using the following equation:

$$BB, \% = \left(\frac{Luc_{act}}{Rel_{rhBMP-2}}\right) \times 100 \quad (4)$$

where, Luc_{act} was defined as luciferase activity obtained by the assay with C2C12 BRE-Luc cell line and the amount of released rhBMP-2 (ng) calculated by the ELISA sandwich method was denominated as $Rel_{rhBMP-2}$. The results were presented in percentage and as Mean ± SEM of triplicates.

2.5.4. In vitro rhBMP-2 release under PEMF

rhBMP-2 was adsorbed by RCPHA, RCPfluidMAG-CT and RCPFeHA and a final concentration of 400 ng/mL was achieved. The rhBMP-2 adsorption and release studies were followed by the previous protocol, as shown in the section "2.5 *In vitro* loading and release of rhBMP-2". The release studies were performed under static and PEMF conditions. The equipment for generation of PEMF is composed of a polymethylmethacrylate tube carrying a home-made Eppendorf support and two solenoids (i.e., Helmholtz coils, the planes of which were parallel). The generated magnetic field and the induced electric field were perpendicular and parallel to the samples, respectively. The Eppendorf's were horizontally introduced into the home-made support and were 5 cm distant from each solenoid plane. A Biostim SPT pulse generator (Igea, Italy) was used to power the solenoids. According to the position of the solenoids and the characteristics of the pulse generator, the electromagnetic stimulus had the following parameters: intensity of the magnetic field equal to 2.0 ± 0.2 mT, amplitude of the induced electric tension equal to 5 ± 1 mV, frequency of 75 ± 2 Hz, and pulse duration of 1.3 ms.

2.6. Statistical analysis

Statistical analyses were performed using GraphPad Prism 5 software. The significant differences in rhBMP-2 loading efficiency, rhBMP-2 release, the effect of microspheres composition on rhBMP-2 release, percentage of rhBMP-2 bioactivity, DNA quantification and expression of osteogenic genes were evaluated by one-way ANOVA with Tukey's multiple comparisons. Values of $p < 0.05$ were accepted as statistically significant.

3. Results

3.1. Physicochemical properties of the microspheres

SEM micrographs of microsphere cross-sections show an inner dense structure in all the tested groups (Fig. 2A–C). RCP presents a smooth inner morphology (Fig. 2A), whereas mineralized microspheres have a

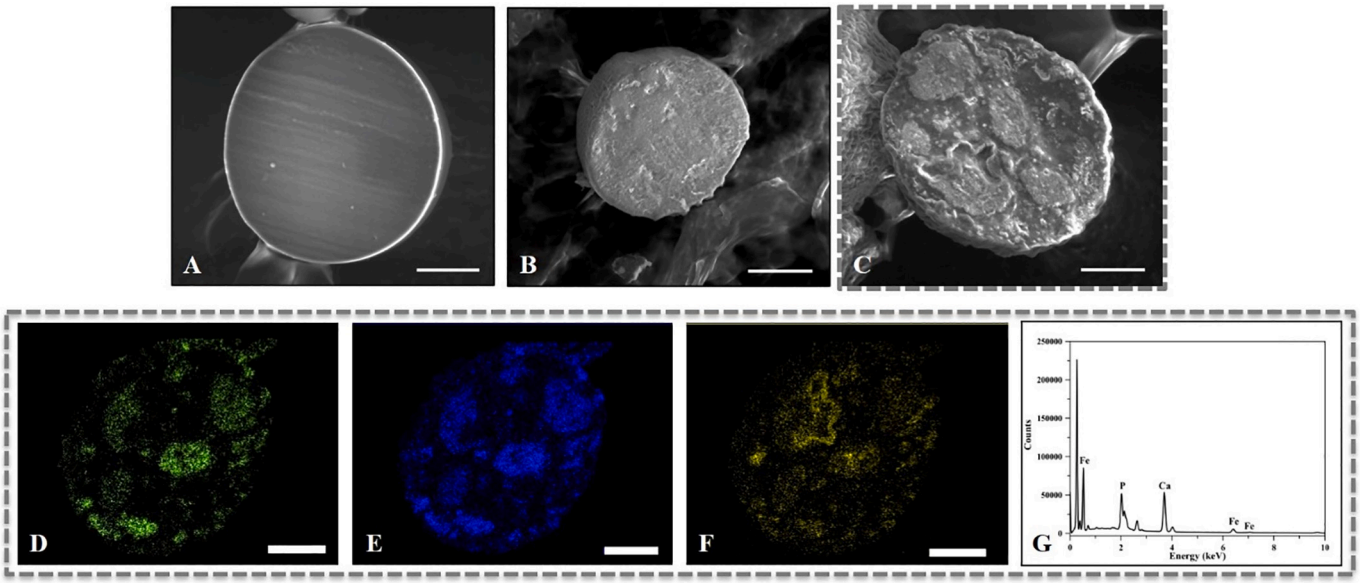

Fig. 2. SEM micrographs of cross-section of the as-synthesized microspheres: A) RCP, B) RCPHA, C) RCPFeHA; SEM micrographs of the distribution of Ca (D), P (E) and Fe (F) in RCPFeHA microspheres; G) EDS microanalysis in RCPFeHA microspheres, (Scale bar: 20 μm).

Table 2
Physical properties of microspheres, (obtained by: [a]zetasizer system; [b]contact angle system; [c]optical micrographs and analysed by Image J software).

Microspheres	Zeta Potential[a], mV	Wettability[b], °	Swelling[c], %
RCP	1.53 ± 0.12	89.87 ± 4.13	16.45 ± 1.62
RCPHA	−3.34 ± 0.05	111.4 ± 0.26	21.22 ± 1.76
RCPFeHA	5.86 ± 0.07	111.9 ± 0.37	43.25 ± 2.27

rougher surface (Fig. 2B, C). Fig. 2D–G shows the distribution maps of Ca, P and Fe, as well as the EDS microanalysis of RCPFeHA, attesting homogeneous distribution of the mineral phase in the microspheres. This is in line with previously reported results. During the biomineralization process of RCP, the mineral phase is chemically linked with the carboxylic groups of RCP matrix that explains the homogeneous distribution of Ca, P and Fe into the mineralized microspheres. Such phase is hydroxyapatite but, in the presence of iron ions, a partial substitution of Ca with Fe ions occurs in the hydroxyapatite structure (FeHA) so to confer superparamagnetic properties with specific magnetisation 1.65 emu/g. Previous investigations of the authors showed that also iron oxide nanoparticles (≈5–25 nm) were nucleated onto the hydroxyapatite nanophase [25,26]. RCPHA and RCPFeHA microspheres show higher surface charge, hydrophobic properties, and higher wettability compared to RCP (Table 2), which can be explained by the presence of mineral phase functionalised with citrate ions [25,26]. The dense polymeric structure limits the wettability in RCP microspheres. On the other hand, the higher wettability of RCPFeHA microspheres can be related to the void spaces generated into the microspheres by the presence of the mineral phase. Mercury intrusion porosimetry reveals the presence of a total porosity of 69.15% in RCPFeHA microspheres.

3.2. Cell viability and in vitro osteogenic activity

In the cell monolayer, the representative optical micrographs and the images obtained by Live/Dead assay indicate high cell viability in the presence of all the tested microspheres after 7 days of cell culture (Fig. 3A–D). In the 3D template configuration, a pellet composed of cells and microspheres formed at one day of cell culture, and cell attachment was confirmed by staining the cell nuclei with DAPI (Fig. 3E). Meanwhile, the 3D templates of RCP, RCPHA and RCPFeHA were stained with Live/Dead (Fig. 3F, G, H) and high cell viability, stained in green, was shown on the microspheres surface, after 1 day of cell culture (Fig. 3F, H). The high fluorescence of RCP material limits the observation of cell nuclei and live&dead cells. The effect of microspheres composition on cell content and cell proliferation was evaluated by DNA content at predetermined time points. Similar cell seeding efficiencies in all the tested microspheres, without significant differences among the groups, were obtained after 2 h of seeding (Fig. 3G). On day 1, a slight decrease in the DNA content was showed in RCPFeHA, due to the cell seeding of Donor 1, increasing again on day 3 and day 7 (Fig. 3G and Supplementary Fig. 1). Taking into account the variability on DNA content among the donors, no statistically significant differences were noted in the DNA content extracted from the cells in contact with all the tested microspheres ($n = 3$) (Fig. 3G and Supplementary Fig. 1).

Osteogenic differentiation of hMSCs was evaluated by the expression of COL I and SPARC genes by real-time PCR. Good levels of osteogenic differentiation are obtained in the presence of all the tested 3D templates after 17 or 21 days of cell culture (Fig. 4A). The results were not statistically different due to the variability of the donors, as showed in the supplementary fig. 2. However, in the donor 1 and 3 the expression of COL I and SPARC were highly expressed in the presence of RCPFeHA microspheres.

3D templates composed of RCP, RCPHA, and RCPFeHA were stained with haematoxylin & eosin. The sections obtained from RCP showed disperse microspheres (example indicated with orange arrow) and cells, while in the presence of mineralized microspheres (i.e. RCPHA and RCPFeHA) highly compact structure was obtained. In both mineralized microspheres, cell nuclei were stained in purple and the produced extracellular matrix or collagen fibers from cells were stained in pink (Fig. 4B, example indicated with blue arrows) and highlighted at a high magnification image for RCPFeHA 3D template (Fig. 4B, example indicated with blue arrows).

3.3. Microspheres loading efficiency

The percentage of loaded rhBMP-2 in all the tested microspheres was higher than 90% as shown in Supplementary Fig. 3A, reaching about 60 ng of rhBMP-2 per milligram of microspheres. In non-mineralized RCP microspheres, a lower percentage of rhBMP-2 (about 94%) was detected, concerning to RCPFeHA microspheres (99.40 ± 0.03%;

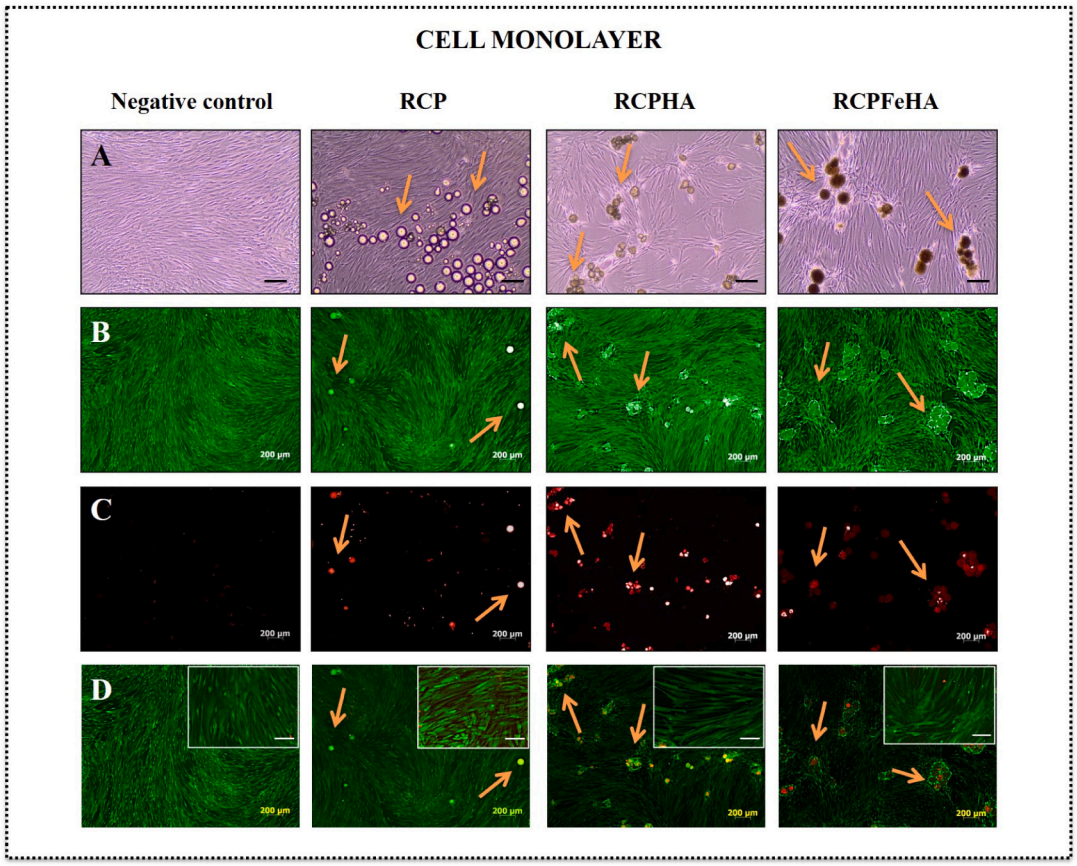

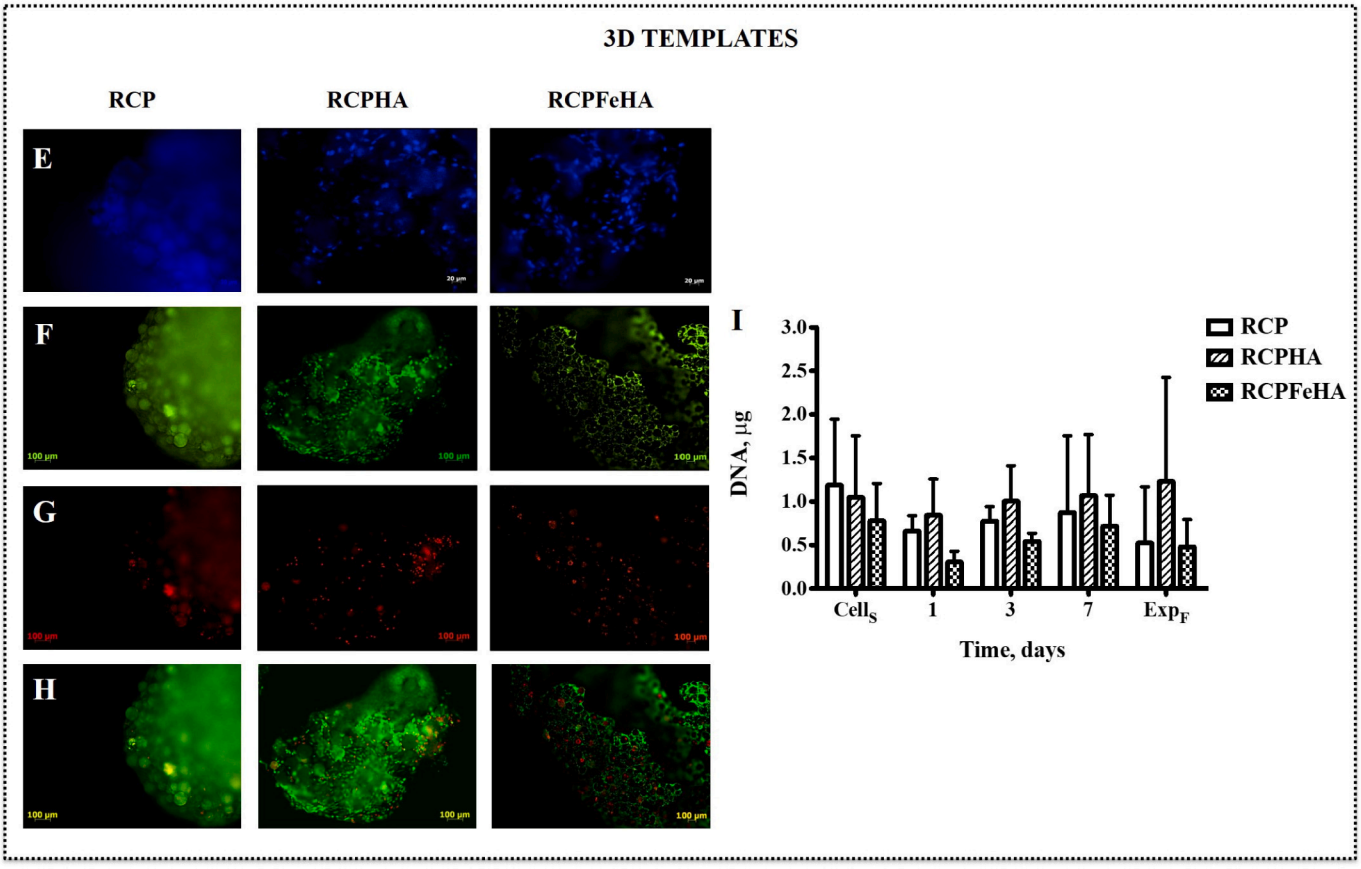

(caption on next page)

Fig. 3. Representative bright-field images (A), Live (B) & dead (C) and merged (D) cells obtained after 7 days of cell culture in presence of cell monolayer of hMSCs and microspheres (examples of microspheres are assigned with orange arrows), (Scale bar: 200 μm (figures), 100 μm (inserts)). 3D templates: cell nuclei stained with DAPI (E), (Scale bar: 20 μm); Live (F) & dead (G) staining and merged images (H) after 1 day of cell culture (Scale bar: 100 μm). (I) hMSCs DNA content in all the tested microspheres, over the course of the experiment (n = 3), ($Cell_S$: cell seeding after 2 h; ExpF: end of experiment 17 days or 21 days, depending on the Donor).

$p < 0.05$). The loading efficiency of microspheres was also evaluated by fluorescence microscopy (Supplementary Fig. 3B). Microspheres presented a very low fluorescent background, whereas the adsorption of texas red labelled rhBMP-2 was detected by the high red fluorescence among the tested microspheres, a concentration of 900 ng/mL (Supplementary Fig. 3B). After the washing steps, the microspheres remained fluorescent, suggesting that at the beginning of the releasing studies, rhBMP-2 was similarly presented in all the tested microspheres (i.e. RCP, RCPHA, and RCPFeHA) (Supplementary Fig. 3B).

3.4. Chemical characterization: rhBMP-2 and microspheres

The interaction of rhBMP-2 with microspheres was evaluated by FTIR analysis. rhBMP-2 presents the typical vibration modes of proteins (i.e. main assignments at 1600, 1560, 1200 cm^{-1}, for Amide *I*, Amide II and Amide III, respectively) (Fig. 5A), and absorption bands in the range of 980–1130 cm^{-1} were related to –COC and –CO stretching [36] (assigned in the Fig. 5A with the symbol: *). By comparing the FTIR spectra of RCP microspheres without and with adsorbed rhBMP-2, no significant differences were obtained in the vibration modes, as shown in Fig. 5A. RCPHA and RCPFeHA microspheres exhibited quite narrow peaks referring to the vibration modes from ≈850 to 1300 cm^{-1} (no rhBMP-2 - Fig. 5B, C). Conversely, in microspheres with adsorbed rhBMP-2, a difference in the stretching phosphate vibration mode ($\nu 3$) (i.e. 1106 and 1036 cm^{-1}) was detected. Particularly, a broadening of the absorption bands in the hybrid (mineralized) microspheres suggests an increase of the crystal disorder induced by rhBMP-2, (rhBMP-2 - Fig. 5B, C). Besides, a chemical shift from 1026 to 1014 cm^{-1} in RCPHA (Fig. 5B) and from 1018 to 1025 cm^{-1} in RCPFeHA (Fig. 5C) was detected, thus suggesting possibly related to chemical interaction with rhBMP-2.

3.5. rhBMP-2 release kinetics and bioactivity

The release kinetics of rhBMP-2 from RCP, RCPHA, and RCPFeHA were measured over 14 days, under agitation mimicking the blood fluid into the human body (Fig. 6A). A burst release for RCP microspheres was obtained, while the slower but sustained release of rhBMP-2 occurred from mineralized microspheres (i.e. RCPHA and RCPFeHA). At 1 h, significant differences in rhBMP-2 release between RCP and RCPHA, between RCP and RCPFeHA (i.e. ****$p < 0.0001$), and between RCPHA and RCPFeHA (i.e. **$p < 0.01$) are observed. After 3 days of the experiment, the complete release of rhBMP-2 from RCP microspheres (900 ng) was achieved, while in RCPHA and RCPFeHA, only ≈42% and ≈17% were respectively released. During the experiment, statistically significant differences were obtained between the tested microspheres ($p < 0.0001$). About 57% (≈460 ng) and 24% (≈200 ng) of rhBMP-2 were released from RCPHA and RCPFeHA microspheres, respectively, after 14 days of investigations (Fig. 6A). After this period, the adsorbed rhBMP-2 in the mineralized microspheres was retrieved by urea treatment and collagenase. Therefore, 5% and 3% of residual rhBMP-2 from RCPHA and RCPFeHA were recovered. Even if all the tested microspheres presented similar rhBMP-2 loading efficiency, physicochemical and morphological properties are relevant parameters for a sustained rhBMP-2 release.

The rhBMP-2 bioactivity was evaluated in the presence of C2C12 BRE-Luc cell line. High rhBMP-2 bioactivity was shown in all the tested microspheres, while statistically significant differences in rhBMP-2 bioactivity were observed between RCPFeHA and RCP microspheres ($p < 0.05$) (Fig. 6B).

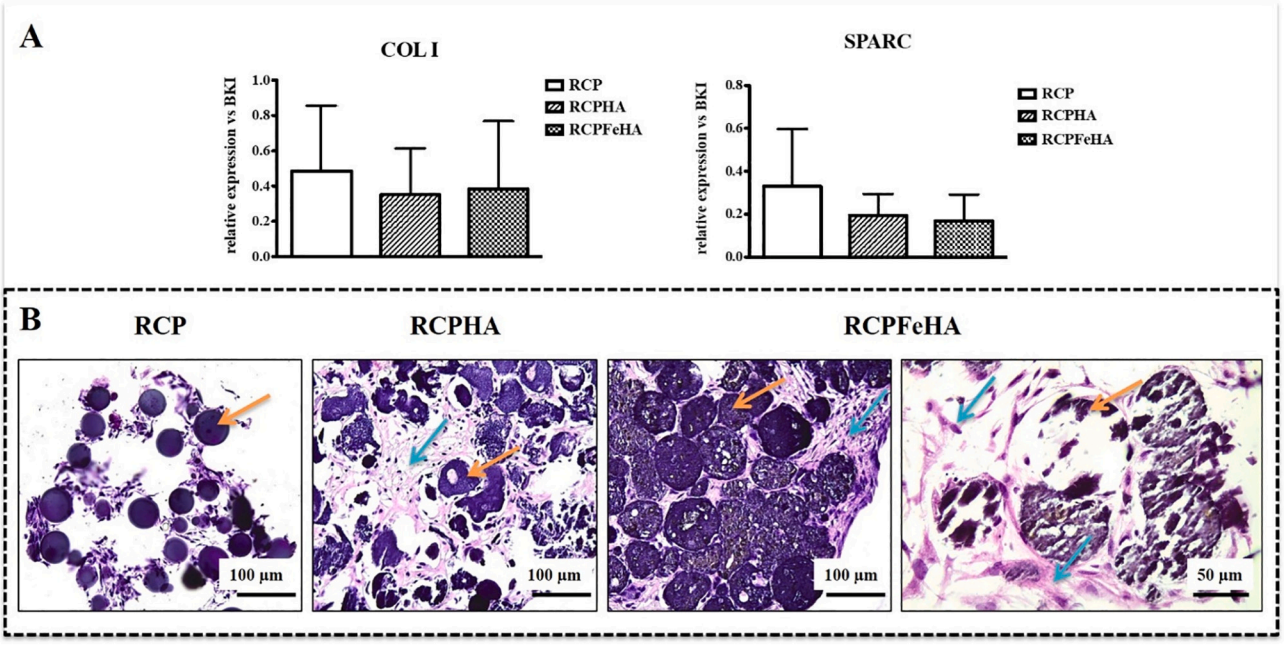

Fig. 4. A) Osteogenic gene expression levels of COL I and SPARC obtained in presence of RCP, RCPHA and RCPFeHA ($n = 3$); B) Haematoxylin and Eosin staining of representative sections of hMSCs cells cultured in osteogenic induction medium with RCP, RCPHA and RCPFeHA microspheres (Orange arrows: example of microspheres in the 3D templates; Blue arrows: extracellular matrix or collagen fibers). (For interpretation of the references to colour in this figure legend, the reader is referred to the web version of this article.)

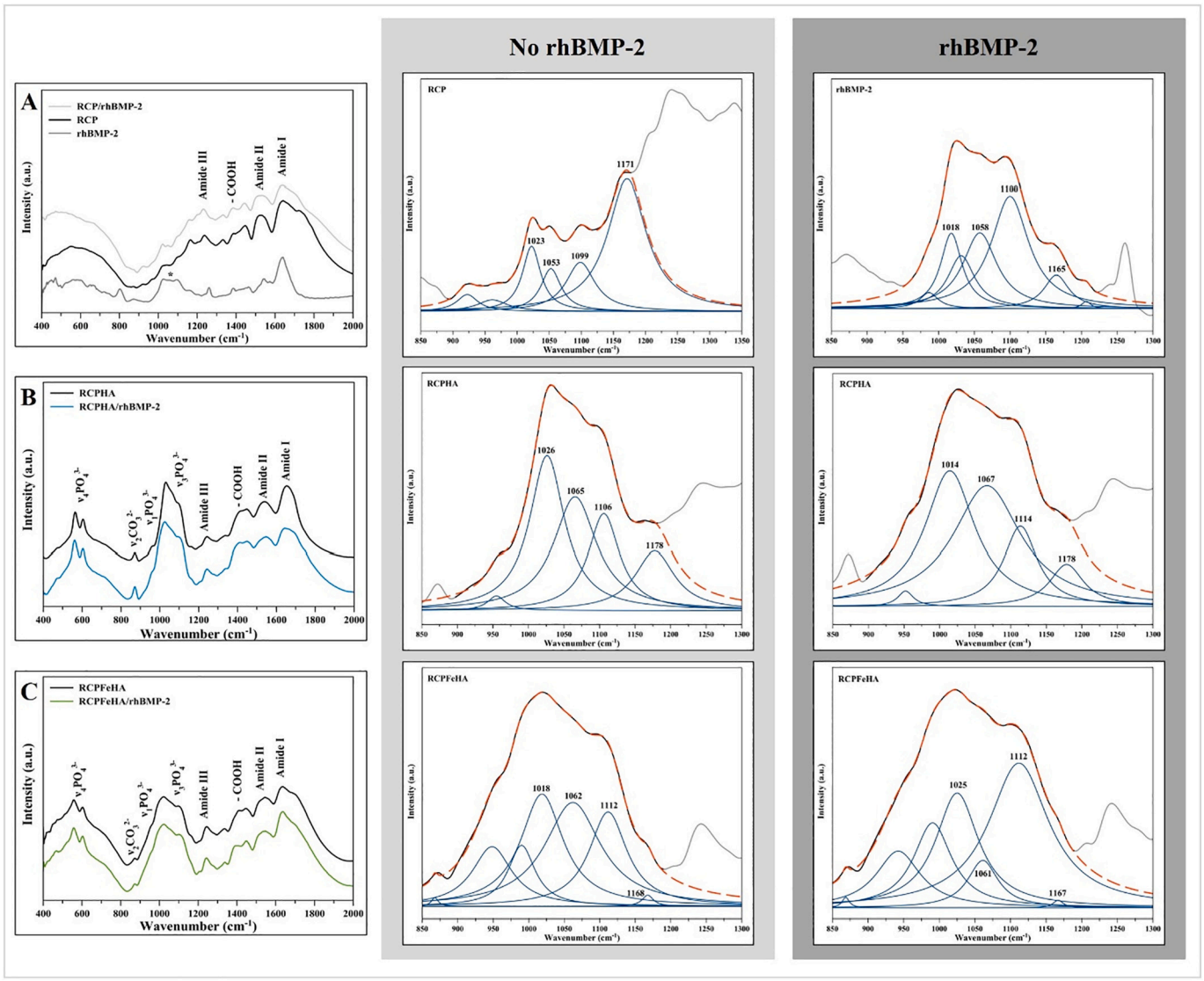

Fig. 5. FTIR vibration peaks of RCP (A), rhBMP-2 (A), RCPHA (B) and RCPFeHA (C) and respective deconvolution peaks in absence or in presence of rhBMP-2. (Orange trace line: Fit by Sum; Black line: FTIR spectra; blue lines: deconvolution peaks). (For interpretation of the references to colour in this figure legend, the reader is referred to the web version of this article.)

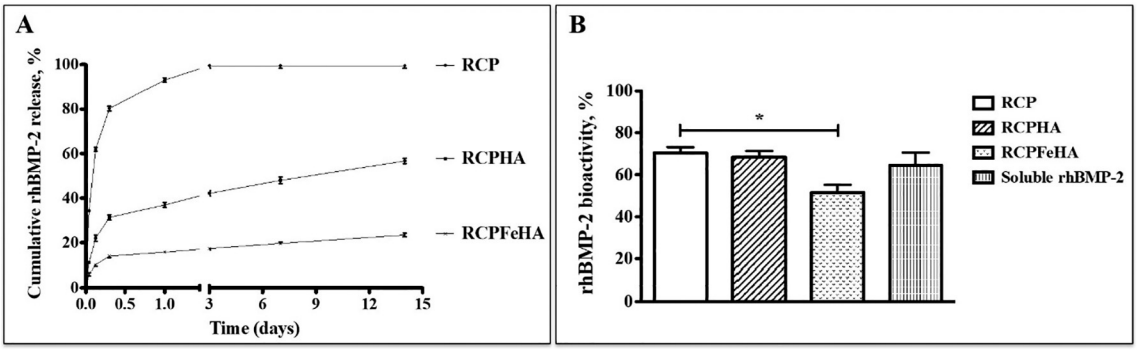

Fig. 6. A) Cumulative rhBMP-2 release (%) from all the as-tested microspheres and B) Released rhBMP-2 bioactivity (%) from RCP, RCPHA and RCPFeHA, (*$p < 0.05$).

3.6. Tuned release of rhBMP-2 using PEMF

rhBMP-2 was adsorbed by RCPHA, RCPfluidMAG-CT and RCPFeHA microspheres and a final concentration of 400 ng/mL was achieved. Release studies were carried out in absence of magnetic stimulation (static, NO PEMF) and under PEMF, for up to 14 days. Static conditions were used as control parameter. In agreement with the results shown in the section "3.5 rhBMP-2 release kinetics and bioactivity", all the tested microspheres were able to release rhBMP-2 over the entire duration of the experiment (Fig. 7A). In RCPHA, no significant differences in the

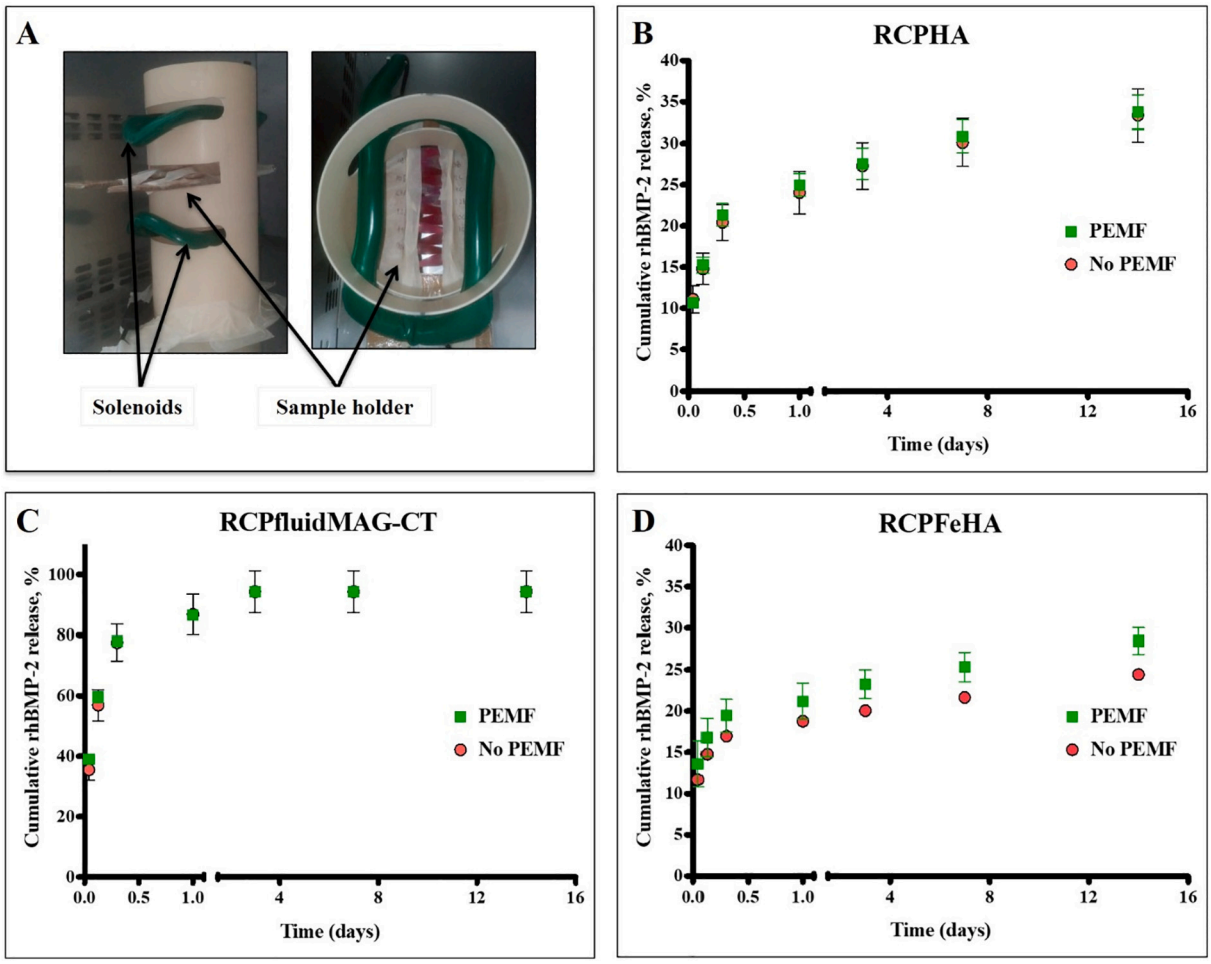

Fig. 7. A) PEMF set-up; Cumulative release of rhBMP-2 (%) from RCPHA (B); from RCPfluidMAG-CT (C) and from RCPFeHA (D) in presence or in absence of PEMF.

release profile at both conditions (i.e. NO PEMF or PEMF) are detected (Fig. 7B). This result is expected, since RCPHA, mineralized with a non-magnetic mineral phase (i.e. the undoped HA) has not super-paramagnetic properties.

The effect of magnetic stimulation on the delivery of rhBMP-2 was analysed with RCPfluidMAG-CT and RCPFeHA microspheres. No significant differences were shown in the rhBMP-2 release profiles from RCPfluidMAG-CT whether or not under PEMF, suggesting that rhBMP-2 was not able to establish a chemical link to the commercial magnetic nanoparticles and a release profile was similar to RCP microspheres (Fig. 6A); therefore they could not exert any stimulating effect on the release of the growth factor (Fig. 7C). fluidMAG-CT are found inside the RCP microspheres that supposedly could limit the interaction with rhBMP-2 due to the bulk structure of the microspheres (Supplementary Fig. 4, identified with green arrows). Conversely, with RCPFeHA microspheres, different rhBMP-2 release profiles were achieved at both conditions (Fig. 7D). Specifically, in NO PEMF the release profile was similar with the result obtained under agitation and shown in section "3.5 rhBMP-2 release kinetics and bioactivity" (reaching about 24%) (Fig. 7A); on the other hand, RCPFeHA microspheres was activated in presence of PEMF and a slight increase on rhBMP-2 release (reaching about 29%) without statistically significant differences was obtained (Fig. 7D). This finding suggests that effective activation of magneto-shaking mechanisms for magnetically controlled release of bioactive molecules can be favoured by establishing a chemical link between the magnetic phases and the molecule to be released.

4. Discussion

Bio-inspired superparamagnetic hybrid microspheres were tested in presence of hMSCs and as carriers and delivery systems for rhBMP-2, to evaluate their potential for application in bone regeneration therapies and, then to assess whether a pulsed electromagnetic field can be effective to control the release profile.

The excellent cytocompatibility and osteogenic ability of hybrid non-magnetic and magnetic microspheres, triggered by bone-like chemical composition, were assessed in 3D templates (composed of donor-derived hMSCs and microspheres). The results report to high cell viability and high density of living cells surrounding the microspheres. Gene expression studies report to the up-regulation of both COL I and SPARC, relevant in the early stage of osteoblastic differentiation, in all the tested microspheres.

At the early stage of MSCs differentiation, stem cells differentiate in pre-osteoblasts and then undergo proliferation, differentiation and induce maturation of extracellular matrix, as indicated by the secretion of genes, such as RUNX2, COL I, ALP, SPP1, SPARC [37,38]. Herein, the gene expression was evaluated at the end of the experiment and we could not conclude which type of microspheres could faster initiate the osteogenesis. We hypothesise that the reduced up-regulation of SPARC is related to the chemical composition of RCPFeHA, showing Fe ions at the surface. In fact, SPARC strongly binds to type I collagen and synthetic apatite and then it could mediate the in vitro mineralization [39,40]. On the other hand, extracellular matrix or collagen fibers mainly formed in presence of RCPFeHA 3D template, as observed in H&E staining. This confirms previous assumptions on the ability of

magnetic materials to improve cell adhesion, proliferation and osteogenic differentiation of human bone marrow stromal cells (hBMSCs) [15].

The magnetic RCPFeHA microspheres were tested in comparison with hybrids with similar but non-magnetic composition and with pure bio-polymeric RCP. The latter shows a compact microstructure and weak interaction with rhBMP-2, so that a burst release profile was detected, that could be disadvantageous for potential adverse biological effects [41].

In previous studies, Mumcuoglu et al. achieved the binding of rhBMP-2 to specific epitopes on porous RCP microspheres and rhBMP-2 release from RCP microspheres, thanks to a controlled crosslinking degree, particle size and pore size [8,42]. Mineralized microspheres show a markedly slower release profile, suggesting that the nanocrystalline mineral apatite phase has a higher affinity with rhBMP-2 and can link it more effectively, thanks to nano-microporous surface topography, and to more active surface chemistry and charge [43–49]. We have found that the rhBMP-2 adsorption on mineralized microspheres is mediated by electrostatic interaction of COO- groups of rhBMP-2 with positively charged Ca^{2+} or Fe^{2+}/Fe^{3+} ions exposed on the apatite surface and through water bridged H-bonds between OH and NH_2 groups of the RCP protein and PO_4^{3-} charge on the apatite surface, as in agreement with the references [45, 50, 51]. Hence, the iron substitution into the apatite structure permitted stronger interaction with rhBMP-2, in comparison with iron-free materials, thus resulting in the slower release of the therapeutic factor and, correspondingly, into reduced bioactivity. This phenomenon can be related to preferred orientations of rhBMP-2 adsorption on the RCPFeHA surface, as described with magnesium apatite surfaces [45]. In our work, we show that a more controlled release profile can be achieved with the iron-doped microspheres, particularly relevant for careful control of the dosage, as needed with the rhBMP-2 factor. Besides the positive effects given by exposure of Fe ions, an additional advantage is offered by the possibility to exploit the superparamagnetic properties of RCPFeHA microspheres that, differently from non-magnetic devices, are sensitive to external magnetic fields. Previous results showed that the magnetic Fe-doped HA phase was effective to modulate the release of anti-cancer drugs, such as doxorubicin or methotrexate [13,52–54]. On the other hand, the release kinetics of rhBMP-2 in magnetic nanogels can be slightly tailored by external magnetic fields [55]. Here, we observe a slight, but definite enhancement in the rhBMP-2 release upon exposure to PEMF. This result could be obtained thanks to the presence of a mineral, highly bioactive magnetic phase (Fe-doped HA), able to chemically link BMP-2, so that the “magneto-shaking” effect induced by the alternate magnetic forces, could be effective. The release extent could be increased by 20% by the application of a field of 2 mT. This preliminary result encourages further investigation in the field, for example by increasing the magnetization of the carrier and/or the applied field/frequency, with the purpose to enhance such a “magnetoshaking” effect. Bone-mimicking materials can better regulate the bone homeostasis and metabolic cell metabolism involved in bone regeneration and remodelling [37,38]. When endowed with magnetic properties, and effective in the remote activation and modulation of release processes or even of hyperthermia, they emerge as a new class of bio-devices promising for safer and personalized therapies in regenerative medicine [2,25,26,56] and cancer therapy [16]. New bio-inspired nanotechnological approaches can thus open to new unpreceded applications, today largely prevented by the cytotoxicity inherent in the current superparamagnetic biomaterials, such as SPIONS [57].

5. Conclusions

Bio-polymeric and hybrid microspheres were investigated as potential rhBMP-2 carriers and delivery systems. The results support the conclusion that hybrid magnetic microspheres are particularly suitable to sustain therapies addressed to bone regeneration, thanks to their osteogenic character and ability to release osteogenic factors in low doses and over a long period. Furthermore, magnetic activation and boosting of drug release is an exciting biofunctionality, promising for new approaches in precision medicine and particularly interesting to sustain tissue healing also in patients affected by reduced endogenous potential, such as the elderly. The development of multifunctional biomaterials with the ability of remote activation is today a relevant research field. In spite, the therapeutic effectiveness of drug-loaded RCPFeHA microspheres has to be validated by more clinically-relevant studies. The obtained results encourage further investigation with the perspective to develop a new smart therapeutic platform to respond to still unmet clinical needs in regenerative medicine and nanomedicine; and to be used as injectable systems, bone cement and scaffolds for local bone replacements.

CRediT authorship contribution statement

TMFP, Conceptualization, Methodology, Validation, Formal analysis, Investigation, Resources, Writing - Original Draft, Writing - Review & Editing; DM, Methodology, Formal analysis, Investigation, Writing - Review & Editing; MM and SP, Supervision, Writing - Review & Editing; JWB, Methodology, Formal analysis, Investigation, Resources, Writing - Review & Editing; SG, Methodology, Formal analysis, Investigation, Writing - Review & Editing; EF, Conceptualization, Formal analysis, Writing - Review & Editing, Supervision, Project administration; SS, Supervision, Project administration, Writing - Review & Editing; SS, EF, MS, AT, Funding acquisition.

Declaration of competing interest

Author Didem Mumcuoglu was employed by the company Fujifilm Manufacturing Europe B.V. The remaining authors declare that the research was conducted in the absence of any commercial or financial relationships that could be construed as a potential conflict of interest.

Acknowledgments

The authors acknowledge to Professor Gerjo van Osch from Department of Orthopaedics, Erasmus MC (Rotterdam, the Netherlands) for the support and research advice, during the secondment in Erasmus MC; to Fujifilm Manufacturing Europe B.V. (The Netherlands) for providing the Cellnest™; to Joachim Nickel from Department for Tissue Engineering and Regenerative Medicine, University Hospital Würzburg, Germany and Fraunhofer IGB, Translational Center Würzburg, Germany, for providing the rhBMP-2; to Andreana Piancastelli and Giulio Boveri from Institute of Science and Technology for Ceramics (ISTEC-CNR), for porosity and contact angle measurements, respectively.

Funding

The research leading to these results has received funding from the European Union Seventh Framework Programme FP7-PEOPLE-2013-ITN under grant agreement n° 607051.

Appendix A. Supplementary data

Supplementary data to this article can be found online at https://doi.org/10.1016/j.msec.2020.111410.

References

[1] Y. Cai, S. Tong, R. Zhang, T. Zhu, X. Wang, In vitro evaluation of a bone morphogenetic protein-2 nanometer hydroxyapatite collagen scaffold for bone regeneration, Mol. Med. Rep. 17 (2018) 5830–5836, https://doi.org/10.3892/mmr.2018.8579.

[2] 3 - Biomineralization process generating hybrid nano- and micro-carriers, in: E. Campodoni, T. Patricio, M. Montesi, A. Tampieri, M. Sandri, S. Sprio, M.L. Focarete, A.B.T.-C.-S.N. for D.D, T. Tampieri (Eds.), Core-Shell Nanostructures Drug Deliv. Theranostics, Woodhead Publishing, 2018, pp. 19–42, , https://doi.org/10.1016/B978-0-08-102198-9.00003-X.

[3] T.-M. De Witte, L.E. Fratila-Apachitei, A.A. Zadpoor, N.A. Peppas, Bone tissue engineering via growth factor delivery: from scaffolds to complex matrices, Regen. Biomater. 5 (2018) 197–211, https://doi.org/10.1093/rb/rby013.

[4] S. Srouji, D. Ben-David, R. Lotan, E. Livne, R. Avrahami, E. Zussman, Slow-release human recombinant bone morphogenetic Protein-2 embedded within electrospun scaffolds for regeneration of bone defect: in vitro and in vivo evaluation, Tissue Eng. Part A. 17 (2010) 269–277, https://doi.org/10.1089/ten.tea.2010.0250.

[5] S. Suliman, Z. Xing, X. Wu, Y. Xue, T.O. Pedersen, Y. Sun, A.P. Døskeland, J. Nickel, T. Waag, H. Lygre, A. Finne-Wistrand, D. Steinmüller-Nethl, A. Krueger, K. Mustafa, Release and bioactivity of bone morphogenetic protein-2 are affected by scaffold binding techniques in vitro and in vivo, J. Control. Release 197 (2015) 148–157, https://doi.org/10.1016/j.jconrel.2014.11.003.

[6] S.Y. Park, S.K. Madhurakkat Perikamana, J.H. Park, S.W. Kim, H. Shin, S.P. Park, H.S. Jung, Osteoinductive superparamagnetic Fe nanocrystal/calcium phosphate heterostructured microspheres, Nanoscale. 9 (2017) 19145–19153, https://doi.org/10.1039/C7NR06777A.

[7] H.Y. Kim, J.H. Lee, J.W. Yun, J.H. Park, B.W. Park, G.J. Rho, S.J. Jang, J.S. Park, H.C. Lee, Y.M. Yoon, T.S. Hwang, D.H. Lee, J.H. Byun, S.H. Oh, Development of porous beads to provide regulated BMP-2 stimulation for varying durations: in vitro and in vivo studies for bone regeneration, Biomacromolecules. 17 (2016) 1633–1642, https://doi.org/10.1021/acs.biomac.6b00009.

[8] D. Mumcuoglu, L. de Miguel, J. Nickel, J.P.T.M. Van Leeuwen, G.J.V.M. Van Osch, S.G.J.M. Kluijtmans, BMP-2 release from synthetic collagen peptide particles, Front. Bioeng. Biotechnol. (2016), https://doi.org/10.3389/conf.FBIOE.2016.01.01596.

[9] G.B. Ramírez Rodríguez, T.M.F. Patrício, J.M. Delgado López, 8 - Natural polymers for bone repair, in: K.M. Pawelec, J.A.B.T.-B.R.B, Second E. Planell (Eds.), Bone Repair Biomater, Second ed., Woodhead Publishing, 2019, pp. 199–232, , https://doi.org/10.1016/B978-0-08-102451-5.00008-1.

[10] H.E. Davis, E.M. Case, S.L. Miller, D.C. Genetos, J.K. Leach, Osteogenic response to BMP-2 of hMSCs grown on apatite-coated scaffolds, Biotechnol. Bioeng. 108 (2011) 2727–2735, https://doi.org/10.1002/bit.23227.

[11] A.-H. Yao, X.-D. Li, L. Xiong, J.-H. Zeng, J. Xu, D.-P. Wang, Hollow hydroxyapatite microspheres/chitosan composite as a sustained delivery vehicle for rhBMP-2 in the treatment of bone defects, J. Mater. Sci. Mater. Med. 26 (2015) 25, https://doi.org/10.1007/s10856-014-5336-8.

[12] L.J. Santos, R.L. Reis, M.E. Gomes, Harnessing magnetic-mechano actuation in regenerative medicine and tissue engineering, Trends Biotechnol. 33 (2015) 471–479, https://doi.org/10.1016/j.tibtech.2015.06.006.

[13] A. Tampieri, M. Sandri, S. Panseri, A. Adamiano, M. Montesi, S. Sprio, Biologically Inspired Nanomaterials and Nanobiomagnetism: A Synergy Among New Emerging Concepts in Regenerative Medicine, Bio-inspired Regen. Med. Mater. Process. Clin. Appl, (2016), pp. 978–981 https://books.google.pt/books?id=NhjYCwAAQBAJ&pg=PR5&lpg=PR5&dq=Biologically+Inspired+Nanomaterials+and+Nanobiomagnetism+:+A+Synergy+among+New+Emerging+Concepts+in+Regenerative+Medicine+1+.+1+The+New+Concept+of+Bio-Inspiration+toward+Biomimetics&source=bl.

[14] F. Heidari, M.E. Bahrololoom, D. Vashaee, L. Tayebi, In situ preparation of iron oxide nanoparticles in natural hydroxyapatite/chitosan matrix for bone tissue engineering application, Ceram. Int. 41 (2015) 3094–3100, https://doi.org/10.1016/j.ceramint.2014.10.153.

[15] Y.P. Guo, T. Long, Z.F. Song, Z.A. Zhu, Hydrothermal fabrication of ZSM-5 zeolites: biocompatibility, drug delivery property, and bactericidal property, J. Biomed. Mater. Res. - Part B Appl. Biomater. 102 (2014) 583–591, https://doi.org/10.1002/jbm.b.33037.

[16] F. Yang, J. Lu, Q. Ke, X. Peng, Y. Guo, X. Xie, Magnetic mesoporous calcium silicate/chitosan porous scaffolds for enhanced bone regeneration and Photothermal-chemotherapy of osteosarcoma, Sci. Rep. 8 (2018) 7345, https://doi.org/10.1038/s41598-018-25595-2.

[17] W. Chen, T. Long, Y.-J. Guo, Z.-A. Zhu, Y.-P. Guo, Magnetic hydroxyapatite coatings with oriented nanorod arrays: hydrothermal synthesis, structure and biocompatibility, J. Mater. Chem. B 2 (2014) 1653–1660, https://doi.org/10.1039/C3TB21769H.

[18] A. Tampieri, T. D'Alessandro, M. Sandri, S. Sprio, E. Landi, L. Bertinetti, S. Panseri, G. Pepponi, J. Goettlicher, M. Banobre-López, J. Rivas, Intrinsic magnetism and hyperthermia in bioactive Fe-doped hydroxyapatite, Acta Biomater. 8 (2012) 843–851, https://doi.org/10.1016/j.actbio.2011.09.032.

[19] V. Iannotti, A. Adamiano, G. Ausanio, L. Lanotte, G. Aquilanti, J.M.D. Coey, M. Lantieri, G. Spina, M. Fittipaldi, G. Margaris, K. Trohidou, S. Sprio, M. Montesi, S. Panseri, M. Sandri, M. Iafisco, A. Tampieri, Fe-doping-induced magnetism in nano-hydroxyapatites, Inorg. Chem. 56 (2017) 4446–4458, https://doi.org/10.1021/acs.inorgchem.6b03143.

[20] M. Iafisco, M. Sandri, S. Panseri, J.M. Delgado, J. Gomez-Morales, A. Tampieri, Magnetic bioactive and biodegradable hollow fe-doped hydroxyapatite coated poly (L-lactic) acid micro-nanospheres, Chem. Mater. 25 (2013), https://doi.org/10.1021/cm4007298.

[21] A. Tampieri, M. Ia, M. Sandri, S. Panseri, C. Cunha, S. Sprio, E. Savini, M. Uhlarz, T. Herrmannsdo, Magnetic Bioinspired Hybrid Nanostructured Collagen − Hydroxyapatite Scaffolds Supporting Cell Proliferation and Tuning Regenerative Process, (2014).

[22] S. Panseri, C. Cunha, T. D'Alessandro, M. Sandri, A. Russo, G. Giavaresi, M. Marcacci, C.T. Hung, A. Tampieri, Magnetic hydroxyapatite bone substitutes to enhance tissue regeneration: evaluation in vitro using osteoblast-like cells and in vivo in a bone defect, PLoS One 7 (2012) 4–11, https://doi.org/10.1371/journal.pone.0038710.

[23] E. Campodoni, A. Adamiano, S. Dozio, S. Panseri, M. Montesi, S. Sprio, A. Tampieri, M. Sandri, Development of innovative hybrid and intrinsically magnetic nanobeads as a drug delivery system, Nanomedicine. 11 (2016) 2119–2130, https://doi.org/10.2217/nnm-2016-0101.

[24] S. Panseri, C. Cunha, T. D'Alessandro, M. Sandri, G. Giavaresi, M. Marcacci, C.T. Hung, A. Tampieri, Intrinsically superparamagnetic Fe-hydroxyapatite nanoparticles positively influence osteoblast-like cell behaviour, J. Nanobiotechnology. 10 (2012) 32, https://doi.org/10.1186/1477-3155-10-32.

[25] T. Patrício, S. Panseri, M. Sandri, A. Tampieri, S. Sprio, New bioactive bone-like microspheres with intrinsic magnetic properties obtained by bio-inspired mineralisation process, Mater. Sci. Eng. C. 77 (2017) 613–623, https://doi.org/10.1016/j.msec.2017.03.258.

[26] T.M. Fernandes Patrício, S. Panseri, M. Montesi, M. Iafisco, M. Sandri, A. Tampieri, S. Sprio, Superparamagnetic hybrid microspheres affecting osteoblasts behaviour, Mater. Sci. Eng. C. 96 (2019) 234–247, https://doi.org/10.1016/j.msec.2018.11.014.

[27] R. De Santis, A. Russo, A. Gloria, U. D'Amora, T. Russo, S. Panseri, M. Sandri, A. Tampieri, M. Marcacci, V.A. Dediu, C.J. Wilde, L. Ambrosio, Towards the design of 3D fiber-deposited poly(ε-caprolactone)/iron-doped hydroxyapatite nanocomposite magnetic scaffolds for bone regeneration, J. Biomed. Nanotechnol. 11 (2015) 1236–1246, https://doi.org/10.1166/jbn.2015.2065.

[28] S. Fahmy-Garcia, M. van Driel, J. Witte-Buoma, H. Walles, J.P.T.M. van Leeuwen, G.J.V.M. van Osch, E. Farrell, NELL-1, HMGB1, and CCN2 enhance migration and vasculogenesis, but not osteogenic differentiation compared to BMP2, Tissue Eng. Part A. 24 (2017) 207–218, https://doi.org/10.1089/ten.tea.2016.0537.

[29] N.H. Dormer, Y. Qiu, A.M. Lydick, N.D. Allen, N. Mohan, C.J. Berkland, M.S. Detamore, Osteogenic differentiation of human bone marrow stromal cells in hydroxyapatite-loaded microsphere-based scaffolds, Tissue Eng. Part A. 18 (2012) 757–767, https://doi.org/10.1089/ten.tea.2011.0176.

[30] L.C. Groeneveldt, C. Knuth, J. Witte-Bouma, F.J. O'Brien, E.B. Wolvius, E. Farrell, Enamel matrix derivative has no effect on the chondrogenic differentiation of mesenchymal stem cells, Front. Bioeng. Biotechnol. 2 (2014) 29, https://doi.org/10.3389/fbioe.2014.00029.

[31] M.J.C. Leijs, G.M. van Buul, E. Lubberts, P.K. Bos, J.A.N. Verhaar, M.J. Hoogduijn, G.J.V.M. van Osch, Effect of arthritic synovial fluids on the expression of immunomodulatory factors by mesenchymal stem cells: an explorative in vitro study, Front. Immunol. 3 (2012) 231, https://doi.org/10.3389/fimmu.2012.00231.

[32] F. Verseijden, H. Jahr, S.J. Posthumus-van Sluijs, T.L. Ten Hagen, S.E.R. Hovius, A.L.B. Seynhaeve, J.W. van Neck, G.J.V.M. van Osch, S.O.P. Hofer, Angiogenic capacity of human adipose-derived stromal cells during adipogenic differentiation: an in vitro study, Tissue Eng. Part A. 15 (2009) 445–452, https://doi.org/10.1089/ten.tea.2007.0429.

[33] B. Blum, C.W. Prince, High-yield Extraction of Osteonductive Agents From Dbm and Methods for Measuring the Same, US 2005/0136124A1, (2005).

[34] B. Herrera, G.J. Inman, A rapid and sensitive bioassay for the simultaneous measurement of multiple bone morphogenetic proteins. Identification and quantification of BMP4, BMP6 and BMP9 in bovine and human serum, BMC Cell Biol. 10 (2009) 20, https://doi.org/10.1186/1471-2121-10-20.

[35] A.M. Brum, J. van de Peppel, C.S. van der Leije, M. Schreuders-Koedam, M. Eijken, B.C.J. van der Eerden, J.P.T.M. van Leeuwen, Connectivity Map-based discovery of parbendazole reveals targetable human osteogenic pathway, Proc. Natl. Acad. Sci. U. S. A. 112 (2015) 12711–12716, https://doi.org/10.1073/pnas.1501597112.

[36] E. Jeevithan, B. Bao, Y. Bu, Y. Zhou, Q. Zhao, W. Wu, Type II collagen and gelatin from silvertip shark (Carcharhinus albimarginatus) cartilage: isolation, purification, physicochemical and antioxidant properties, Mar. Drugs. 12 (2014) 3852–3873, https://doi.org/10.3390/md12073852.

[37] D. Lopes, C. Martins-Cruz, M.B. Oliveira, J.F. Mano, Bone physiology as inspiration for tissue regenerative therapies, Biomaterials. 185 (2018) 240–275, https://doi.org/10.1016/j.biomaterials.2018.09.028.

[38] A. Rutkovskiy, K.-O. Stensløkken, I.J. Vaage, Osteoblast differentiation at a glance, Med. Sci. Monit. Basic Res. 22 (2016) 95–106, https://doi.org/10.12659/MSMBR.901142.

[39] N. Ribeiro, S.R. Sousa, R.A. Brekken, F.J. Monteiro, Role of sparc in bone remodeling and cancer-related bone metastasis, J. Cell. Biochem. 115 (2014) 17–26, https://doi.org/10.1002/jcb.24649.

[40] D. de Melo Pereira, P. Habibovic, Biomineralization-inspired material design for bone regeneration, Adv. Healthc. Mater. 7 (2018) 1–18, https://doi.org/10.1002/adhm.201800700.

[41] L. Xiong, J. Zeng, A. Yao, Q. Tu, J. Li, L. Yan, Z. Tang, BMP2-loaded hollow hydroxyapatite microspheres exhibit enhanced osteoinduction and osteogenicity in large bone defects, Int. J. Nanomedicine 10 (2015) 517–526, https://doi.org/10.2147/IJN.S74677.

[42] D. Mumcuoglu, L. de Miguel, S. Jekhmane, C. Siverino, J. Nickel, T.D. Mueller, J.P. van Leeuwen, G.J. van Osch, S.G. Kluijtmans, Collagen I derived recombinant protein microspheres as novel delivery vehicles for bone morphogenetic protein-2, Mater. Sci. Eng. C. 84 (2018) 271–280, https://doi.org/10.1016/j.msec.2017.11.031.

[43] H. Zhou, T. Wu, X. Dong, Q. Wang, J. Shen, Adsorption mechanism of BMP-7 on hydroxyapatite (001) surfaces, Biochem. Biophys. Res. Commun. 361 (2007) 91–96.

[44] X. Dong, Q. Wang, T. Wu, H. Pan, Understanding adsorption-desorption dynamics of BMP-2 on hydroxyapatite (001) surface, Biophys. J. 93 (2007) 750–759, https://doi.org/10.1529/biophysj.106.103168.

[45] B. Huang, Y. Yuan, T. Li, S. Ding, W. Zhang, Y. Gu, C. Liu, Facilitated receptor-recognition and enhanced bioactivity of bone morphogenetic protein-2 on magnesium-substituted hydroxyapatite surface, Sci. Rep. 6 (2016) 24323, https://doi.org/10.1038/srep24323.
[46] W.J. King, P.H. Krebsbach, Growth factor delivery: how surface interactions modulate release in vitro and in vivo, Adv. Drug Deliv. Rev. 64 (2012) 1239–1256 http://www.sciencedirect.com/science/article/pii/S0169409X12001007.
[47] P. Zhou, J. Wu, Y. Xia, Y. Yuan, H. Zhang, S. Xu, K. Lin, Loading BMP-2 on nanostructured hydroxyapatite microspheres for rapid bone regeneration, Int. J. Nanomedicine 13 (2018) 4083–4092, https://doi.org/10.2147/IJN.S158280.
[48] F. Gilde, O. Maniti, R. Guillot, J.F. Mano, D. Logeart-Avramoglou, F. Sailhan, C. Picart, Secondary structure of rhBMP-2 in a protective biopolymeric carrier material, Biomacromolecules. 13 (2012) 3620–3626, https://doi.org/10.1021/bm3010808.
[49] D. Schwartz, S. Sofia, W. Friess, Integrity and stability studies of precipitated rhBMP-2 microparticles with a focus on ATR-FTIR measurements, Eur. J. Pharm. Biopharm. 63 (2006) 241–248, https://doi.org/10.1016/j.ejpb.2005.12.011.
[50] H. Autefage, F. Briand-Mésange, S. Cazalbou, C. Drouet, D. Fourmy, S. Gonçalvès, J.P. Salles, C. Combes, P. Swider, C. Rey, Adsorption and release of BMP-2 on nanocrystalline apatite-coated and uncoated hydroxyapatite/β-tricalcium phosphate porous ceramics, J. Biomed. Mater. Res. - Part B Appl. Biomater. 91 (2009) 706–715, https://doi.org/10.1002/jbm.b.31447.
[51] E. Quinlan, E.M. Thompson, A. Matsiko, F.J. O'Brien, A. Lopez-Noriega, Long-term controlled delivery of rhBMP-2 from collagen-hydroxyapatite scaffolds for superior bone tissue regeneration, J. Control. Release 207 (2015) 112–119, https://doi.org/10.1016/j.jconrel.2015.03.028.
[52] M. Iafisco, C. Drouet, A. Adamiano, P. Pascaud, M. Montesi, S. Panseri, S. Sarda, A. Tampieri, Superparamagnetic iron-doped nanocrystalline apatite as a delivery system for doxorubicin, J. Mater. Chem. B 4 (2016) 57–70, https://doi.org/10.1039/C5TB01524C.
[53] S. Sprio, M. Sandri, M. Iafisco, S. Panseri, M. Montesi, A. Ruffini, A. Adamiano, A. Ballardini, A. Tampieri, Nature-inspired Nanotechnology and Smart Magnetic Activation: Two Groundbreaking Approaches Toward a New Generation of Biomaterials for Hard Tissue Regeneration, Adv. Tech. Bone Regen, (2016), https://doi.org/10.5772/63229.
[54] S. Sarda, M. Iafisco, P. Pascaud-Mathieu, A. Adamiano, M. Montesi, S. Panseri, O. Marsan, C. Thouron, A. Dupret-Bories, A. Tampieri, C. Drouet, Interaction of folic acid with Nanocrystalline Apatites and extension to methotrexate (Antifolate) in view of anticancer applications, Langmuir. 34 (2018) 12036–12048, https://doi.org/10.1021/acs.langmuir.8b02602.
[55] M. Fan, J. Yan, H. Tan, Y. Miao, X. Hu, Magnetic biopolymer nanogels via biological assembly for vectoring delivery of biopharmaceuticals, J. Mater. Chem. B 2 (2014) 8399–8405, https://doi.org/10.1039/C4TB01106F.
[56] A. Adamiano, M. Iafisco, M. Sandri, M. Basini, P. Arosio, T. Canu, G. Sitia, A. Esposito, V. Iannotti, G. Ausanio, E. Fragogeorgi, M. Rouchota, G. Loudos, A. Lascialfari, A. Tampieri, On the use of superparamagnetic hydroxyapatite nanoparticles as an agent for magnetic and nuclear in vivo imaging, Acta Biomater. 73 (2018) 458–469, https://doi.org/10.1016/j.actbio.2018.04.040.
[57] A. Farzin, M. Fathi, R. Emadi, Multifunctional magnetic nanostructured hardystonite scaffold for hyperthermia, drug delivery and tissue engineering applications, Mater. Sci. Eng. C. 70 (2017) 21–31, https://doi.org/10.1016/j.msec.2016.08.060.

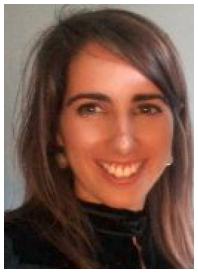

Tatiana M. Fernandes Patrício is PhD Integrated Researcher, Postdoc, and member of the scientific board of the CDRSP-Polytechnic Leiria, PT. She has been participated in PT and EU projects (FCT, ANI, FP7, H2020). She has been attended to numerous international conferences, as oral speaker, is author or co-author of scientific papers, chapters, co-author of 2 national patents, invited as reviewer of scientific journals, tutoring several young researchers and she won 2 awards (Marie Curie Research Fellowship; Doctor Europaeus). Main interest areas: biomaterials, magnetic biomaterials, in vitro cell studies, tissue engineering, biomedical devices; bone regeneration, additive biomanufacturing, IDI projects.

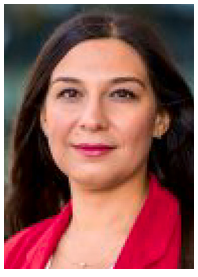

Didem Mumcuoglu started her PhD in Netherlands in 2014. Her PhD study was funded by Marie Curie ITN (Bioinspire) involving Fujifilm and Erasmus Medical Center as project partners. Her role in the consortium was to develop a growth factor delivery system for bone regeneration under supervision of Dr. Sebastiaan Kluijtmans and her PhD promoter Prof. Gerjo van Osch. After finishing her PhD she started as a post-doc in Prof. Patricia Danker's group. Her current research is focused on designing a device based on supramolecular polymers for islet cell transplantation.

Monica Montesi is researcher at Institute of Science and Technology for Ceramics of the National Research Council, ISTEC-CNR (Faenza, Italy) in Bioceramics and Bio-hybrid Composites Group coordinated by Dr. A. Tampieri. Lab Manager of Cellular and Molecular Biology Lab.

Areas of interest and Research Skills

• Molecular and cellular biology
• Regenerative medicine, tissue engineering and nanomedicine
• Biological evaluation of cell/material interactions
• 2D and 3D cell culture in static and dynamic (Bioreactor) conditions.

Silvia Panseri is researcher at Institute of Science and Technology for Ceramics of the National Research Council, ISTEC-CNR (Faenza, Italy).

Areas of interest and Research Skills

- Tissue engineering, nanotechnology and regenerative medicine.
- Cell/biomaterial interactions.
- 3D cell culture using biomaterials.
- Advanced cell and molecular biology techniques.

Janneke Witte-Bouma is a research technician. She currently works in Rotterdam at ErasmusMC, department of Oral and Maxillofacial Surgery. She has participated in research projects and is co-author of scientific papers. Main interest areas: molecular biology, cell biology, biomaterials, in vitro cell studies, tissue engeneering and bone regeneration.

Shorouk Fahmy Garcia has PhD in Life Sciences, Regenerative Medicine and Biotechnology. A highly experienced and multi-skilled biomedical specialist with extensive experience in cellular & molecular biology. A result-driven, strongly motivated professional with a sharp, analytical mind aiming to contribute to global health developing accessible therapies. Extensive work experience in different environments with a thorough understanding of the R&D pipeline. Refined interpersonal skills with good ability to build long-lasting professional relationships. Passionate about medical innovations, communication, and public health.

Monica Sandri is Researcher at the Institute of Science and Technology for Ceramics - National Research Council of Italy (ISTEC-CNR). Skills: synthesis methodologies, forming methods to produce prototypes, investigation of the relations between micro- nano-structural properties and material performance. Development of biomineralization processes towards nanostructured hybrid biomimetic composites for the development of 3D porous scaffold aimed to the regeneration of bone, osteochondral and periodontal tissue. Polymeric functionalized hydrogels and scaffolds, obtained through blending processes, for the regeneration of not mineralized tissue like cardiac tissue, tendon, ligament, cartilage. Bioactive biomimetic and superparamagnetic nanoparticles and hybrid beads as drug delivery systems.

Anna Tampieri is the Director of Research at ISTEC-CNR. 30 years of experience in material science, particularly for the development of new ceramic and hybrid biomaterials and of new processes based on biomineralization and biomorphic transformation for the realization of biomimetic devices for regenerative medicine and nanomedicine. Author of over 250 scientific papers (H-index = 49) and inventor of 17 national and international patents. Coordinator of various EC-funded and National projects. Scientific consultant of various biomedical and pharma companies, she was creator and founder of 2 innovative start-ups, and she translated 7 products from the lab to the market.

Eric Farrell is the head leader of the Bone Tissue Engineering research laboratory (Erasmus Medical Centre, Netherlands, Rotterdam) that performs basic and translational research with the main aim of investigating how to modulate new bone formation and the various cellular interactions that occur during this process. The research is focused on the process of endochondral ossification as a promising avenue for the generation of clinically relevant quantities of bone tissue to repair large bone defects. Fields of expertise: Bone tissue engineering, endochondral ossification, osteoimmunology, stem cells and bone metastasis.

Simone Sprio is a senior researcher and scientific responsible for the research line: Bioceramics for regenerative medicine, at ISTEC-CNR. Over 20 years of experience in the development of new ion-doped calcium-phosphate-based nanomaterials, and new processes based on low-temperature consolidation and biomorphic transformation, for the development of porous 3-D scaffolds and injectable pastes/bone cements with superior bioactivity, anti-infectious ability and mechanical properties, addressed to the regeneration of critical size, load-bearing bone regions. Author of about 150 peer reviewed papers (H-index = 26) and inventor of 8 granted patents. Responsible or WP Leader in various EC-funded and National research projects.